kinetic motion of the ions is 0.0185 joules/cm² per shot; an additional 0.0015 joules/cm² per shot is present in ionization energy. The combined energy density is 0.020 joules/cm² per shot compared with the total energy density of 0.026 joules/cm² per shot given by the calorimeter. Although the two results are within experimental error, the higher figure given by the calorimeter could be attributed to fast neutrals.

Conclusions

The agreement between the energy density inferred from the ion probe results and the energy density measured with a calorimeter shows that the ion probe can give quantitative information in a tenuous nitrogen plasma having a directed energy of a few hundred electron volts. The simplicity and compact size of the ion probe, with or without an analyzing grid, makes it ideal for probing the exhaust plasmas from pulsed plasma guns.

References

[1] Stuhlinger, E., "Electric propulsion—1964," Astronaut. Aeronaut. **2**, 26 (1964).

[2] Longmire, C. L., "The use of plasma for propulsion of interplanetary rockets," pp. 3-11; Starr, W. L. and Naff, J. T., "Acceleration of metal-derived plasmas," pp. 47–59; Marshall, J., "Hydromagnetic plasma gun," pp. 60–72; Gartenhaus, S. and Tannenwald, L. M., "Propulsion from pinch collapse," pp. 73–78, *Plasma Acceleration*, edited by S. W. Kash (Stanford Univ. Press, Stanford, Calif., 1960).

[3] Larson, A. V., Gooding, T. J., Hayworth, B. R., and Ashby, D. E. T. F., "An energy inventory in a coaxial plasma accelerator driven by a pulse line energy source," AIAA J. **3**, 977–979 (1965).

[4] Duclos, D. P., Aronowitz, L., Fessenden, F. P., and Carstensen, P. B., "Diagnostic studies of a pinch plasma accelerator," AIAA J. **1**, 2505–2513 (1963).

[5] Gooding, T. J., Hayworth, B. R., and Lovberg, R. H., "Use of ballistic pendulums with pulsed plasma accelerators," ARS J. **32**, 1599 (1962).

[6] Coensgen, F. H., Sherman, A. E., Nexsen, W. E., and Cummins, W. P., "Plasma injection into a magnetic field of cusped geometry," Phys. Fluids **3**, 764 (1960).

[7] Ashby, D. E. T. F., "The flow of high energy plasma in a magnetic guide field," Proc. Intern. Conf. Ionization Phenomena Gases, 6th, Paris **4**, 465–468 (1963).

[8] Moore, D. and Kinzie, P., "Diagnostics of the space charge neutralization of ion beams by electron injection," *AIAA Progress in Astronautics and Rocketry: Electrostatic Propulsion*, edited by David B. Langmuir, Ernst Stuhlinger, and J. M. Sellen, Jr. (Academic Press Inc., New York, 1961), Vol. 5, pp. 457–471.

[9] McDaniel, E. W., *Collision Phenomena in Ionized Gases* (John Wiley and Sons, Inc., New York, 1964), pp. 629–658.

Dynamic Response of an Encased Elastic Cylinder with Ablating Inner Surface

J. D. Achenbach*

Northwestern University, Evanston, Ill.

Introduction

THE loss of mass and stiffness affects the dynamic response of a structure. Previous work in this area[1] is related to re-entry problems, where the stiffness of the thin covering layer of ablative material is neglected, and only the influence of the mass loss is taken into account. In studying the dynamic response of a burning cylindrical-grain in a solid-propellant rocket, the influence of the stiffness of the solid-propellant material cannot be ignored. The present note is a study of the forced vibrations of an encased elastic cylinder with an ablating inner surface.

A time-dependent internal pressure is applied at the inner surface of the cylinder. If the cylinder were of a compressible elastic material the problem would concern cylindrical waves that emanate from the moving inner surface and interact with the surrounding shell. Since the ablation rate is very small as compared to the dilatational wave velocity, a vibrationary type of response would set in after a short time. In this note the cylinder material is assumed to be incompressible. As a consequence, the wave velocity of dilatational waves is infinite, and a forced vibration is immediately started without initial wave effects. It may be mentioned that solid-propellant materials show very high bulk moduli and are usually considered incompressible.

Special attention has been devoted to the circumferential stress at the ablating inner surface. The analysis is valid for arbitrary ablation rates.

Statement of the Problem

A long elastic cylinder is considered with a circular port of monotonically increasing radius $a(t)$ and a constant outer radius b at which the cylinder is bonded to a thin elastic shell. Both the cylinder and the surrounding shell are maintained in a state of plane strain.

If the cylinder is under the action of an internal pressure the equation of motion is expressed as

$$\partial\sigma_r/\partial r + (\sigma_r - \sigma_\theta)/r = \rho_p(\partial^2 u/\partial t^2) \tag{1}$$

In Eq. (1) r and θ are the polar coordinates, and u is the displacement in the radial direction. The subscript p denotes a material constant of the cylinder.

For an incompressible elastic cylinder the radial displacement is of the form

$$u = k(t)/r \tag{2}$$

where $k(t)$ is a function of t only.

Let s_{ij} and e_{ij}, respectively, denote the components of deviatoric stress and strain. The stress-strain relation for the incompressible elastic material can then be expressed in the form

$$s_{ij} = 2\mu e_{ij} \tag{3}$$

From Eq. (3) we derive

$$\sigma_r - \sigma_\theta = 2\mu(\epsilon_r - \epsilon_\theta) = -4\mu k(t)/r^2 \tag{4}$$

The radial stress is prescribed at $r = a(t)$ as

$$r = a(t): \quad \sigma_r = -\sigma_i(t) \tag{5}$$

The radial stress at $r = b$ is derived from the equation of motion of an element of the thin surrounding shell. With the requirements that the radial stress and the circumferential strain are continuous at the cylinder shell interface, we obtain

$$[\sigma_r]_{r=b} = -(h/b)\,(E'/b^2)\,k(t) - \rho_s\,(h/b)\,\ddot{k}(t) \tag{6}$$

In Eq. (6), $E' = E_s/(1 - \nu_s^2)$, and ν_s is Poisson's ratio. A subscript s denotes a material constant of the shell (case). The thickness of the case is denoted by h.

The expressions for u and $\sigma_r - \sigma_\theta$, respectively Eqs. (2) and (4), are now substituted into Eq. (1), and the resulting equation for σ_r is subsequently integrated with respect to r. Taking into account that the radial stress is prescribed at the ablating inner surface Eq. (5) and at $r = b$ Eq. (6), we obtain the following differential equation for $k(t)$:

$$\left\{\rho_p \ln\left[\frac{b}{a(t)}\right] + \rho_s\left(\frac{h}{b}\right)\right\}\ddot{k}(t) - \left\{2\mu\left[\frac{1}{b^2} - \frac{1}{a(t)^2}\right] - \left(\frac{h}{b}\right)\frac{E'}{b^2}\right\}k(t) = \sigma_i(t) \tag{7}$$

Received October 26, 1964. This work was supported by the Office of Naval Research under Contract ONR Nonr. 1228(34) with Northwestern University.

* Assistant Professor, Department of Civil Engineering. Member AIAA.

The solution of Eq. (7) is subject to the initial conditions

$$k(t) = \dot{k}(t) = 0 \qquad \text{for} \qquad t \leq 0 \tag{8}$$

For convenience a number of dimensionless quantities are introduced. We define

$$\tau = t/t_f \qquad a(\tau) = a_0\alpha(\tau) \qquad K(\tau) = k(\tau)/b^2 \tag{9}$$

In Eq. (9) t_f is the total burning time. The ablation function $\alpha(\tau)$ runs from $\alpha(0) = 1$ to $\alpha(1) = b/a_0$.

The governing equation (7) can then be rewritten as

$$\ddot{K}(\tau) + \zeta^2\chi(\tau)K(\tau) = \varphi(\tau) \tag{10}$$

in which

$$\chi(\tau) = \frac{(h/b) - 2(\mu/E')[1 - (b/a_0)^2/\alpha(\tau)^2]}{(h/b) + (\rho_p/\rho_s)\ln[(b/a_0)/\alpha(\tau)]} \tag{11}$$

$$\varphi(\tau) = \frac{\zeta^2\sigma_i(\tau)/E'}{(h/b) + (\rho_p/\rho_s)\ln[(b/a_0)/\alpha(\tau)]} \tag{12}$$

and ζ is a dimensionless burning time defined as

$$\zeta = t_f(E'/\rho_s)^{1/2}/b \tag{13}$$

Inspection of Eqs. (11) and (12) reveals that the parameters in the present problem are the structural parameters (h/b) and (b/a_0), the material parameters (ρ_p/ρ_s) and (μ/E'), the ablation function $\alpha(\tau)$, and the burning time ζ.

Method of Solution

From Eq. (13) it is noticed that ζ is a large real parameter. Ordinary differential equations of the type Eq. (10) with φ a large parameter can be solved by Horn's method.[2] The solution that is obtained by Horn's method is in the form of a series in descending powers of ζ, which are asymptotic to exact solutions of the differential equation uniformly in a region of τ. Since ζ is very large, we neglect all terms of orders lower than and equal to $(1/\zeta)$. Using Horn's method[2] the two independent complementary solutions of Eq. (10) are found as

$$K_1(\tau) = \chi(\tau)^{-1/4}\exp\left[i\zeta\int_0^\tau \chi(s)^{1/2}ds\right] + 0\,\frac{1}{\zeta} \tag{14}$$

$$K_2(\tau) = \chi(\tau)^{-1/4}\exp\left[-i\zeta\int_0^\tau \chi(s)^{1/2}ds\right] + 0\,\frac{1}{\zeta} \tag{15}$$

It is easy to check that the Wronskian of the solutions $K_1(\tau)$ and $K_2(\tau)$ equals $2i\zeta$. Using a well-known theorem the solution of the inhomogeneous Eq. (10), subject to the initial conditions Eq. (8), can then be written as

$$K(\tau) = \frac{1}{2i\zeta}\int_0^\tau [K_1(\tau)K_2(\xi) - K_2(\tau)K_1(\xi)]\varphi(\xi)d\xi \tag{16}$$

After substitution of $K_1(\tau)$ and $K_2(\tau)$ into Eq. (16) the resulting expression for $K(\tau)$ is simplified by introduction of the new variable

$$v = \int_0^\xi \chi(s)^{1/2}ds \tag{17}$$

We obtain

$$K(\tau) = \frac{1}{\zeta}\chi(\tau)^{-1/4}Im\left\{\left[\exp\left(i\zeta\int_0^\tau \chi(s)^{1/2}\,ds\right)\right]\times \int_0^{v_1}\psi(v)e^{-i\zeta v}\,dv\right\} \tag{18}$$

in which

$$v_1 = \int_0^\tau \chi(s)^{1/2}\,ds \tag{19}$$

$$\psi(v) = \chi[s(v)]^{-3/4}\varphi[s(v)] \tag{20}$$

An advantageous feature of the integration over v in Eq. (18) is that the exponential $\exp[-i\zeta v]$ contains the very large real parameter ζ. Integrals containing such an exponential are suited for evaluation by the method of stationary phase.[2] The method of stationary phase entails that the real integral is replaced by a contour integral along the lines $v = -iw$ and $v = v_1 - iw$, where w runs from 0 to ∞. Since ζ is a large real parameter the exponential $\exp(-\zeta w)$ dies out very rapidly and the main contributions to the integral come from near $v = 0$ and $v = v_1$. We find

$$K(\tau) = \zeta^{-2}\chi(\tau)^{-1}\varphi(\tau) - \zeta^{-2}\chi(0)^{-3/4}\varphi(0)\chi(\tau)^{-1/4}\times \cos\left[\zeta\int_0^\tau \chi(s)^{1/2}ds\right] + O\frac{1}{\zeta} \tag{21}$$

It is noticed that the first term of Eq. (21) is the quasi-static solution for $K(\tau)$. The second term gives the dynamic deviations from the quasi-static solution. The frequency of the vibrations is increasing with time since $\chi(s)$ is a positive function. In the present analysis we assume that $\sigma_i(0+) \neq 0$, i.e., the internal pressure is applied as a step function. Higher-order terms of $(1/\zeta)$ have to be taken into account if the internal pressure increases gradually.

Of special interest is the circumferential stress at the ablating inner surface $r = a(\tau)$. With Eq. (4) and the condition on the radial stress at $r = a(\tau)$, the circumferential stress can be expressed as

$$\sigma_\theta[a(\tau), \tau] = -\sigma_i(\tau) + 4\mu(b/a_0)^2\alpha(\tau)^{-2}K(\tau) \tag{22}$$

From the designer's point of view the maximum and the minimum values of the circumferential stress are of particular importance. These stress envelopes are found as

$$\sigma_\theta[a(\tau), \tau]_{\min}^{\max} = \sigma_{\theta\text{quasi-static}} \pm \sigma_\theta^*(\tau) \pm O(1/\zeta) \tag{23}$$

in which

$$\sigma_\theta]_{\text{quasi-static}} = -\sigma_i(\tau) + 4\mu(b/a_0)^2\zeta^{-2}\alpha(\tau)^{-2}\chi(\tau)^{-1}\varphi(\tau) \tag{24}$$

$$\sigma_\theta^*(\tau) = M\sigma_i(0+)[\chi(0)/\chi(\tau)]^{1/4}\alpha(\tau)^{-2} \tag{25}$$

where

$$M = 4(b/a_0)^2/[(h/b)(E'/\mu) - 2 + 2(b/a_0)^2] \tag{26}$$

The influence of the material and the structural parameters on the dynamic response of the encased cylinder is clearly shown by the solutions Eqs. (21–23). It is of note that

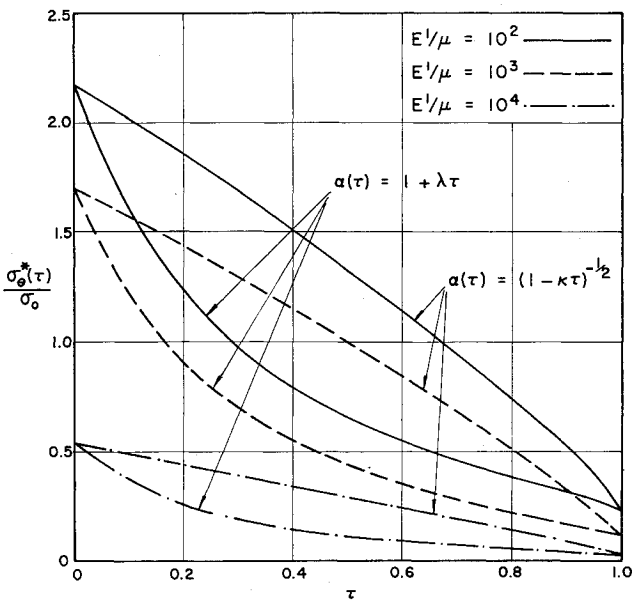

Fig. 1 Amplitude of the circumferential overstress at the ablating inner surface for $\sigma_i(\tau) = \sigma_0 H(\tau)$.

the burning time t_f does influence the periods of the vibrations, but it does not affect the amplitudes.

As a conclusion the influence of (E'/μ) and $\alpha(\tau)$ on the amplitudes of the dynamic part of the circumferential stress is shown in Fig. 1. Two ablation functions are considered

$$\alpha(\tau) = (1 - \varkappa\tau)^{-1/2} \qquad \text{where} \qquad \varkappa = 1 - (a_0/b)^2 \quad (27)$$

and the linear function

$$\alpha(\tau) = 1 + \lambda\tau \qquad \text{where} \qquad \lambda = (b/a_0) - 1 \quad (28)$$

In both cases (E'/u) has values 10^4, 10^3, and 10^2. The other parameters are chosen as

$$b/a_0 = 3 \qquad h/b = 1/200 \qquad \rho_p/\rho_s = 1/5 \quad (29)$$

and

$$\sigma_i(\tau) = \sigma_0 H(\tau) \quad (30)$$

References

[1] Tasi, J., "Effect of mass loss on the transient response of a shallow spherical sandwich shell," AIAA J. 2, 58–64 (1964).

[2] Jeffreys, H., *Asymptotic Approximations* (Oxford University Press, London, 1962), p. 39 and 52.

A Model for Low-Pressure Extinction of Solid Rocket Motors

R. F. CHAIKEN*
Aerojet-General Corporation, Azusa, Calif.

Nomenclature

Rocket-chamber parameters

A_b = propellant burning area
A_t = nozzle-throat area
C_D = nozzle-discharge coefficient
P_c = chamber pressure
P_{cr} = critical chamber pressure for onset of "low-frequency" instability
P_e = extinction chamber pressure
V_c = chamber volume
L^* = V_c/A_t

Propellant parameters

r = propellant burning rate
n = steady-state burning rate pressure exponent, $r = cP^n$
ρ_p = propellant density
P_{DL} = low-pressure stable deflagration limit
M = average molecular weight of gaseous combustion products
T_f = adiabatic flame temperature of propellant
T_g = a temperature parameter that is approximated by the adiabatic flame temperature of the ammonium perchlorate monopropellant flame
k_g = rate constant for the ammonium perchlorate monopropellant flame reactions, $k_g = A_g \exp(-E_g/RT_g)$

Miscellaneous parameters

g = gravitation constant
R = gas constant
t = time
τ = critical time constant

Received October 21, 1964. This work was supported in part by Aerojet-General Corporation, Solid Rocket Research and Development Division, and in part by the Advanced Research Projects Agency under Contract No. AF49(638)-851 monitored by the Air Force Office of Scientific Research.

* Technical Consultant.

Introduction

ANDERSON, Strehlow, and Strand[1] have shown that vacuum firings of solid-propellant rocket motors using regressive burning grains exhibit a low-pressure burning limit that is generally higher than the low-pressure stable deflagration limit of the propellant as determined in a Crawford bomb strand burner. Their studies with ammonium perchlorate composite propellant with varying aluminum content suggest that the extinction pressure (P_e), although independent of burning geometry, is strongly dependent upon Al content and motor L^* (ratio of chamber volume to nozzle-throat area). Their data could be curve-fitted by an expression of the form

$$L^* = A(P_e)^{-\alpha} \quad (1)$$

where the constants A and α varied with Al content.

For nonaluminized propellant, the value of the exponent α was approximately twice the value of the steady-state burning pressure exponent (n) at the pressure P_e. In this case, Eq. (1) becomes almost identical to theoretical expressions derived by Akiba and Tanno,[2] Sehgal and Strand,[3] and Cohen[4] for describing the critical pressure (P_{cr}) for onset of "low-frequency" combustion instability, i.e.,

$$L^* = A'(P_{cr})^{-2n} \quad (2)$$

The theoretical derivations considered the instability as arising from a coupling between the lag of burning-rate response due to the propellant thermal gradient and the lag in exhausting the chamber due to nozzle flow.

The strong resemblance between the theoretical and empirical expressions suggested to these authors[1, 3, 4] that the critical pressure for onset of unstable burning (i.e., P_{cr}) should correspond to the observed extinction pressure (i.e., P_e). However, there are two serious discrepancies that arise from this approach: 1) the value of α for the case of aluminized propellants (8–16%) is much greater than $2n$, and 2) the extinction pressure is zero for an infinite L^*. Since in a Crawford bomb, L^* can be construed as approaching infinity, it might be expected that P_e should have a limiting value approaching the low-pressure stable deflagration limit. Although it has been argued[1, 3, 4] that aluminum or its solid combustion product might in some way affect the propellant thermal response or the nozzle-exhaust time, no adequate quantitative explanation of these discrepancies has been offered.

It is the purpose of this note to offer a possible explanation in terms of a new model for the extinction process. This new approach suggests that Eq. (2) defines criteria for possible temporary extinguishment rather than permanent extinguishment, and, as such, P_{cr} should not be identified with P_e of Eq. (1). In addition, the model enables the derivation of a theoretical P_e vs L^* relationship that differs considerably from the form of Eq. (1).

Model of Rocket Extinction

It is first assumed that solid composite propellants exhibit a low-pressure stable deflagration limit (P_{DL}) that is independent of their extinction under conditions of rocket motor venting. Such phenomena have apparently been noted in strand burners (Crawford bomb) where, below a minimum inert gas bomb pressure, strand burning cannot persist. Low-pressure deflagration limits have been reported as high as 400 psia for some ammonium nitrate propellants[5] and as low as 6 psia for some ammonium perchlorate (AP) propellants. Even ammonium perchlorate monopropellant strands exhibit a P_{DL}.[6]

A detailed discussion of the causes for a P_{DL} in solid composite propellants is outside the scope of the present paper; however it can be noted that Friedman[6] and Nachbar[7] attempted to explain the P_{DL} of AP strands in terms of radiation heat loss from the burning surface. Also, it would